The 2015 World Congress on
Aeronautics, Nano, Bio, Robotics, and Energy (ANBRE15)
Incheon, Korea, August 25-28, 2015

Investigation of Two-Axis Synchronous Accuracy of Plate Pivot Control under Various Poses of Industrial Dual-Arm Robot for Ball-Rolling Motion on Working Plate

* Yuichi HORIZUMI[1)], Wei WU[2)], Toshiki HIROGAKI[3)] and Eiichi AOYAMA[4)]

[1), 2), 3), 4)] *Department of Mechanical Engineering Doshisha University, Japan*
[1)] duo0515@mail4.doshisha.ac.jp; [2)] weiwu@mail.doshisha.ac.jp
[3)] thirogak@mail.doshisha.ac.jp; [4)] eaoyama@mail.doshisha.ac.jp

ABSTRACT

New applications continue to emerge to control not only linear motion but also rotational motion in high accuracy manufacturing fields. Dual-arm industrial robots have been gaining attention as novel tools in automation. We therefore focus on using them to flexibly control both the linear motion and the rotational motion of a working plate. However, it is difficult to measure the synchronous accuracy of two rotary axes of a working plate. The working plate uses dual-arm cooperative control to keep the ball rolling in a circular path on it. In the present report, we estimate the effect of the synchronous accuracy of two rotary axes under upper and lower poses to support the working plate and avoid ball-rolling error. We also discuss a method to improve the robot motion accuracy based on the double ball bar (DBB) method to generate a robot on-line program by teaching the playback method in industrial fields. In particular, we discussed the error of rolling motion in case of teaching the order angle by chopping wave.

1. INTRODUCTION

Recently, developers of machining tools are paying more and more attention to multi-joint dual-arm robots, and as a result it is expected that the robot will reclaim its place in the field of new automation [1]. The expanding range of applications for 5-axis machining centers, parallel mechanisms, and new industrial robots has created a need for faster and more accurate control of complex rotational motions for adjusting the position of tables [2–3]. Improved accuracy for such motions essentially requires better measurement and evaluation technology [4]. To determine the accuracy of contour motion, it is necessary to evaluate the accuracy of the synchronization of two or more control axes. Consequently, there have been many studies done on the accuracy of synchronous motion, such as studies using the double ball bar (DBB) method for

---

[1)] Corresponding Author
[2), 3), 4)] Professor

systems with two translational axes and one rotational axis [5–9]. However, most of these studies have included translational axis movement, and very few have dealt with the synchronous motion accuracy of rotational axes alone. Furthermore, there have been no examples of application to new types of industrial robots that require advanced coordinated operation of two arms, such as dual-arm robots. The double ball bar (DBB) method has been used to test the accuracy of arbitrary two-axis synchronous control that includes straight-line motion. That method evaluated the accuracy of two-axis synchronous control by measuring the extension and con- traction of an elastic bar that is equipped with a scale for measuring the distance between two points. However, that principle does not allow for measurement on translational axes where there is no movement. Highly accurate gyro-sensors, such as those used on aircraft, can be considered for measuring the accuracy of two-axis synchronous control. However, such sensors are large and heavy, so cannot be used for compact robots. They are also expensive and not suited for on-site use. There is therefore a need for a system that can easily evaluate motion accuracy in factories or at other work sites.

Recently, the dual-arm robot uses developed multi-joint robot arms to demonstrate that two robot arms can hold a working plate to form a closed link structure to maintain some support rigidity that is practical in work and has a similar operation range to that of humans. The two arms of a dual-arm robot holding a working plate can move the plate in a relatively high degree of freedom space with linear and rotational motions. We therefore propose a new method for simple on-site detection of motion error in two-axis synchronous rotational motions of rotation axis. That method causes a ball to roll in a circular path on a working plate and detects rolling motion error relative to a reference circle. Simulations and experiments both confirmed the effectiveness and practicality of that method. We also elucidated the relation of motion error detection sensitivity to the moment of inertia of the rolling ball and presented guidelines for selecting the ball to match the required plate rotation. We additionally explained the characteristics by using DBB for when the center of two-axis rotational motion axis is the same as the center of the rolling motion of the ball and when there is an offset angle error in the rotational motion of rotation axis 6.

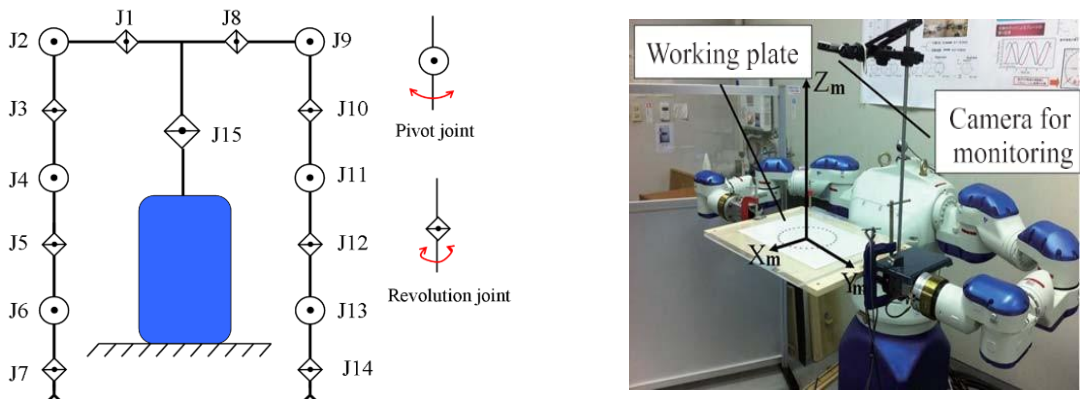

(a).Definition of Ji. (b).Definition of coordinate.

Fig. 1. Dual-arm robot.

2. EXPERIMENTAL EQUIPMENT

We used the robot (**Fig. 1(a),(b)**) in this experiment. The robot used in this experiment was Yaskawa Corporation's Motoman DIA 10, which is a dual-arm robot featuring 15 degrees of freedom. The robot has a 98 kgf (10 kg) payload per arm, 1,100 mm horizontal reach per arm (forming the centerline of the base rotation to the tool mounting surface), and a repeatability of ±0.1 mm. It is roughly the same size as a human, and the robot arms can synchronously work together on one task to double the pay-load. The two manipulators can also be used independently.

3. SIMULATION OF ROLLING MOTION

3.1 Moti Simulation of ball rolling motion on a working plate

The dual-arm is operated around the X_m and Y_m-axis, as shown in Fig.1 (a), in synchronized motion to control the plate. We gave a circular motion order to the robot using the technique of the DBB method [4–5]. This technique focuses on attention to the known motion error of translational two-axis movement. We assumed the coordinate system fixed in space is Σ_R, angular velocity of the center of circular motion of radius R is ω, time is t and initial phase is θ_0. We used the positioning order of moving straight on two orthogonal axes (e.g., the X_R-axis and Y_R-axis) and gave the motion order for one axis as sine function Rsinωt, the other axis cosine function Rcosωt {that is to say Rsin(ωt + 90◦)} to diagnose the motion error. The technique that some authors have suggested pays attention to when the ball rolls on the plate and does circular motion. When we think about the ball, one pivot axis is sine function θ_0 sinωt, the other angle order (maximum tilting angle is θ_0, $0<\theta_0<90◦$) is cosine function θ_0 cosωt, and the error between the practical rolling trace of the ball and the standard orbit can be considered for measuring the accuracy of the two-axis synchronous control. This technique is an absolute standard in gravity by rolling motion; we fell down in comparison with sliding and the motion continued until the frictional force was small and then the technique became highly sensitive.

We considered a 3-dimensional model (**Fig. 2(a)**); the center of the plate is the origin of the coordinates. Therefore, we applied a 2-dimensional model of rolling motion for a ball on a slope such as (**Fig. 2(b)**), the X_m and Y_m-axis run downward along the slope, and the Z_m-axis is perpendicular to this. θ is the angle of rotation around the Y_m-axis of the plate in the horizontal plane, and is positive in the counter clock wise (CCW) direction.

The plate does not have a guide and can theoretically exercise six degrees of freedom. For convenience, we used the motion coordinate system for this moving body. Here, minus Z is the direction of gravitation of the coordinate systems, Σ_m was fixed at the plate, and Σ_B was fixed at the center of gravity position of the object (the Z_m-axis is perpendicular to the contact surface of the plate). ${}_mX_B$ and ${}_mY_B$ look at Σ_B from Σ_m. θ_0 the maximum angle. The mass of the ball is M, the radius of ball is r and the ball revolution angle around the center is ϕ. By considering gravity, the motion equation of the center of gravity of the ball is as follows:

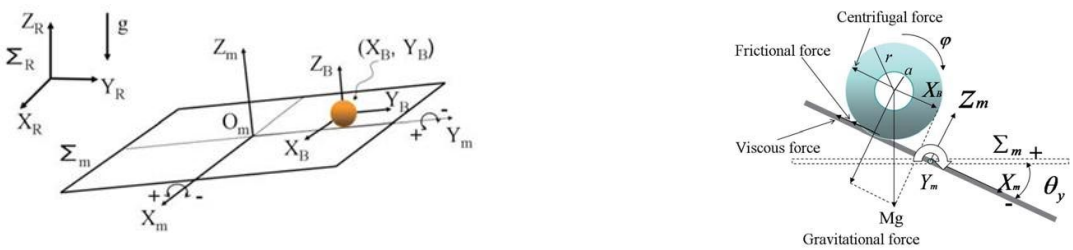

(a).Three dimensional coordinates. (b). Sectional view in two dimensional coordinates.

Fig. 2. Model of ball rolling on working plate.

$$M\frac{d^{2m}X_B}{dt^2} = \mathrm{Mgsin\theta} - f - D\frac{d^m X_B}{dt} - M^m X_B\left(\frac{d\theta}{dt}\right)^2 \tag{1}$$

Here, the mass of ball is M and we assume that the viscous force, and its damping coefficient D are in proportion to the velocity of the center of the ball, frictional force f at the contact point between the ball and the plate surface, and the centrifugal force of the ball when the plate is turning. Here, the centrifugal force is found to be essential to improve the accuracy of the simulation including the non-steady response various considerations. On the other hand, the equation of rolling motion around the center of gravity is

$$I\frac{d^2\varphi}{dt^2} = rf \tag{2}$$

Here, I is the inertia moment around the ball center, and we transform Eq. (2) to

$$f = \frac{I}{r}\frac{d^2\varphi}{dt^2} \tag{3}$$

From Eqs. (1) and (3) we obtained the following equation

$$M\frac{d^{2m}X_B}{dt^2} = \mathrm{Mgsin\theta}_y - \frac{I}{r}\frac{d^2\varphi}{dt^2} - D\frac{d^m X_B}{dt} - M^m X_B\left(\frac{d\theta}{dt}\right)^2 \tag{4}$$

Here, we assumed there is no sliding motion when the ball rolls on the plate. Then, we have the relationship as described in Eq. (5).

$$M\frac{d^m X_B}{dt} = r\frac{d\varphi}{dt} \tag{5}$$

We obtained Eq. (6) by differentiating Eq. (5)

$$\frac{d^{2m}X_B}{dt^2} = r\frac{d^2\varphi}{dt^2} \tag{6}$$

As previously mentioned, we so far have thought about only a true solid ball, not a hollow ball. Furthermore in this paper, the difference in density takes into account different balls to improve generality. Here, the inertia moment of the hollow ball with a constant density is I. From Eqs. (6) and (4), the motion equation of the rolling ball on the sloping plate is

$$\frac{7r^5 - 5a^3r^2 - 2a^5}{5(r^3 - a^3)r^2} M\frac{d^{2m}X_B}{dt^2} = \mathrm{Mgsin}\theta_y - D\frac{d^mX_B}{dt} - M^mX_B\left(\frac{d\theta_y}{dt}\right)^2 \tag{7}$$

Here we assumed

$$I_e = \frac{7r^5 - 5a^3r^2 - 2a^5}{5(r^3 - a^3)r^2} \quad , \quad D_M = \frac{D}{M}$$

$$I_e\frac{d^{2m}X_B}{dt^2} = \mathrm{g}\sin\theta_y - D_M\frac{d^mX_B}{dt} - M^mX_B\left(\frac{d\theta_y}{dt}\right)^2 \tag{8}$$

Thus, we have equation as Eq. (8).

The force acting on the ball is considered to be due to the slant of the plate. We assumed that the angle θ of the plate is a function of time t, and the plate center is fixed when the plate is rotating by dual-arm manipulation. Here, the circular motion is in the X_m-Y_m plane; when we looked at it the Z_m-X_m or Z_m-Y_m plane, we could surmise that it caused each rotation to have simple harmonic oscillation. Therefore, when we operated the plate by robot, the phase of angle of rotation angle θ(t) led to a movement of 90 degrees together with the X_m-axis rotation and Y_m-axis rotation. Here, α is the initial phase angle, and we set α = 90◦, and $\theta_{x0} = \theta_{y0}$, which means $\varepsilon = 1$, caused the circular orbit of the ball on a plate by 14-axis (J1～J14 in Fig. 1) synchronous control. The equation [10] of ball rolling on the X_m -Y_m plane of the working plate is as follows:

$$I_e\begin{bmatrix}\frac{d^{2m}X_B}{dt^2}\\ \frac{d^{2m}Y_B}{dt^2}\end{bmatrix} = \mathrm{g}\begin{bmatrix}\theta_y\\ \theta_x\end{bmatrix} - D_M\begin{bmatrix}\frac{d^mX_B}{dt}\\ \frac{d^mY_B}{dt}\end{bmatrix} - \begin{bmatrix}{}^mX_B\left(\frac{d\theta_y}{dt}\right)^2\\ {}^mY_B\left(\frac{d\theta_y}{dt}\right)^2\end{bmatrix} \tag{9}$$

$$\theta_y(t) = \theta_{y0}\sin(\omega t) \tag{10}$$

$$\theta_x(t) = \theta_{x0}\cos\omega t = \theta_{x0}\sin[\omega t + \alpha] = \varepsilon\theta_{y0}sin[\omega t + \alpha] \tag{11}$$

In addition, to maintain the same damping coefficient, we put a 5 mm thick acrylic board on the wooden construction plate. The flatness of this acrylic board is ±0.003 mm. In this report, we performed the experiment and simulation with various balls to improve

generality. The specifications of ball are shown in **Fig. 3**, and we used the M22 ball this time.

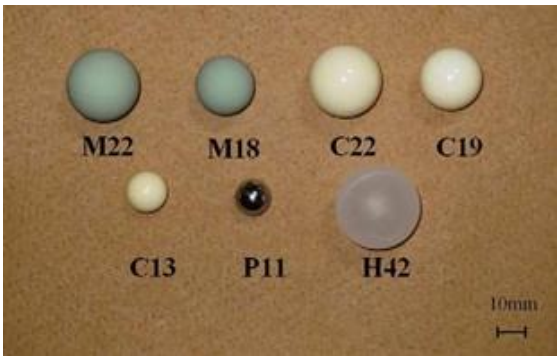

Fig. 3. Balls used in experiment and simulation.

3.2 Control Model

We considered the ball's motion equation in the X_m-Y_m plane in Section x.y and in this section and designed a control system for controlling the ball's motion. The power action on the ball is the plate's slant. Therefore, we assumed its power act is $F_{Ball} = 5/7Mg\theta$. The ball's motion in X_m-Y_m axis was the same, which is the point of a simple harmonic oscillation. Here we only considered the X_m-axis. We transformed Eq. (8), assumed the ball's velocity is ${}^mV_B$, and got the state's equation:

$$\begin{bmatrix} \frac{d^mV_B}{dt} \\ \frac{d^mX_B}{dt} \end{bmatrix} = \begin{bmatrix} -D_M & -\frac{5}{7}\left(\frac{d\theta_y}{dt}\right)^2 \\ 1 & 0 \end{bmatrix} \begin{bmatrix} {}^mV_B \\ {}^mX_B \end{bmatrix} + \begin{bmatrix} 1/M \\ 0 \end{bmatrix} F_{Ball} \tag{12}$$

Then we did a Laplace-transform on it:

$$s^mV_B(s) + {}^mV_B(0) = -D_M{}^mV_B(s) - \frac{5}{7}\left(\frac{d\theta_y}{dt}\right)^2 {}^mX_B(s) + \frac{1}{M}F_{Ball}$$

$$s^mX_B(s) + {}^mX_B(0) = {}^mV_B(s) \tag{13}$$

4. ANALYTICAL AND EXPERIMENTAL RESULTS AND DISCUSSION

4.1 Controlling Motion error and converting it into angle error under various postures

We discussed about the posture of the robot. We had performed a DBB experiment about motion error with a robot with symmetrical posture. However, we had not performed an experiment about motion error with a robot with changing working

plate height. We performed a DBB experiment to improve the motion accuracy by teaching angle. First, we considered the robot arm. The arms of dual-arm robots were constructed with master-arms and slave-arms as shown in **Fig.4**.

Therefore, it is thought that the movement does not fall in line with each arm even if they are moved by the same robot. By considering the motion accuracy of each arm, we focused on angle error. By considering the motion accuracy of each arm, we focused on angle error. Here, it is necessary to convert the motion error into angle error. We defined the maximum measurement error ΔR_{max} and the minimum measurement error ΔR_{min} as shown in **Fig.5**. Fig.5 suggests that a difference of the ΔR_{min} of the left-right arm influences it because of the quantity of the backlash (Y_R- Z_R plane) around the Y_m-axis that appears in the opposite direction to the X_m-axis circumference (X_R- Z_R plane).

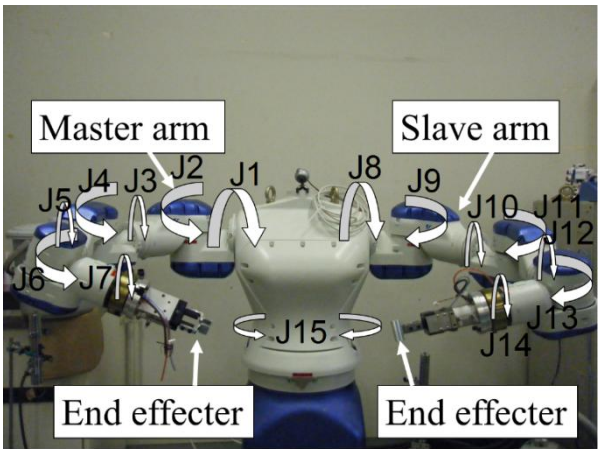

Fig. 4. Structure of a robot arms.

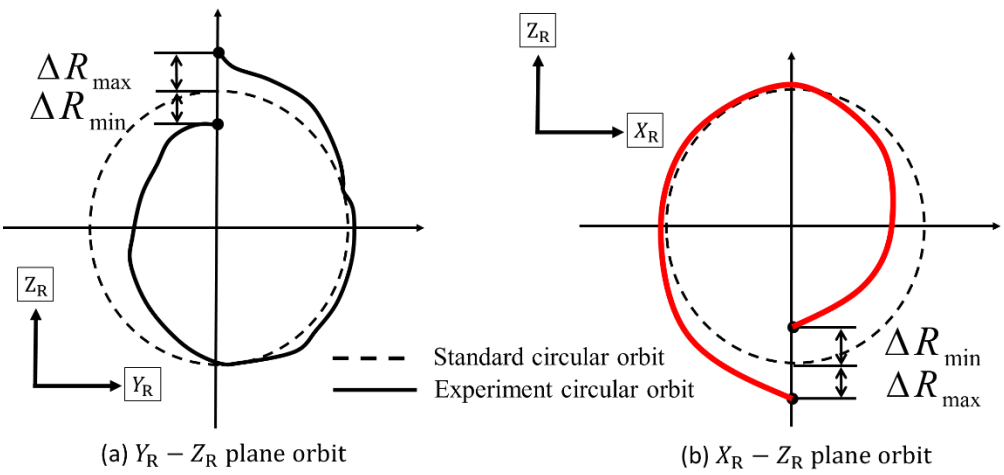

Fig. 5. Definition of ΔR_{max} and ΔR_{min}.

The converted maximum measurement error of the left arm is θ_{lmax} and that of the right arm is θ_{rmax}. The synthetic error of the arms is θ_{max}, the length of DBB is l, and the expression to convert motion error into angle error is shown in Eq. (14) and (15).

$$\Delta\theta_{lmax} = \mathrm{Arc}\sin\left(\frac{D_{lmax}}{l}\right) \tag{14}$$

$$\Delta\theta_{rmax} = \mathrm{Arc}\sin\left(\frac{D_{rmax}}{l}\right) \tag{15}$$

In addition, the synthetic error expression of each arm is as follows.

$$\Delta\theta_{max} = \Delta\theta_{lmax} + \Delta\theta_{rmax} \tag{16}$$

We discuss about the angle error using these Eq.

4.2 Rolling motion error of dual-arm robot under various postures

By considering the motion accuracy of each arm, we focused on angle error. This time we attempt changing the height to 100 mm from the standard posture at the basic height of the robot arm and the state for DBB evaluation. The results are shown in **Fig. 6**. The experiment by the DBB method fixed the position of the right arm, and arc interpolation allows you to exercise CW and CCW. I sent the order for circular motion with a radius of 100mm and changed the speed to 500 mm/min chopping fine from 500 mm/min to 2000 mm/min and tested the robot. In addition, regarding the plane coordinates that the Z_R-axis is related to compared with a previous study, I know that a particular discontinuous error will be produced on the Z_R-axis. Therefore, I mainly considered the plane coordinates that the Z_R-axis was related to as a laboratory finding. The specific example of the result is shown in **Fig. 7**. We fixed the right arm in the Z_R-X_R plane and sent it, and we fixed the right arm in the Z_R-X_R plane as shown in Fig. 7 (a),(b). Arc interpolation allows you to send an order in the case when you are allowed to move in 500 mm/min. The case when arc interpolation was allowed to be used for exercise in relation to a posture of one arm hanging as a specific example below 2000 mm/min in the Z_R-Y_R plane is shown in Fig. 7 (c),(d).

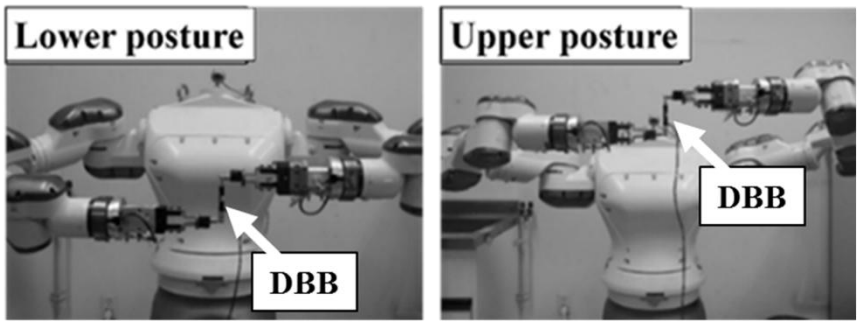

(a) DBB test under lower posture (b) DBB test under upper posture

Fig. 6. Setup for DBB evaluation.

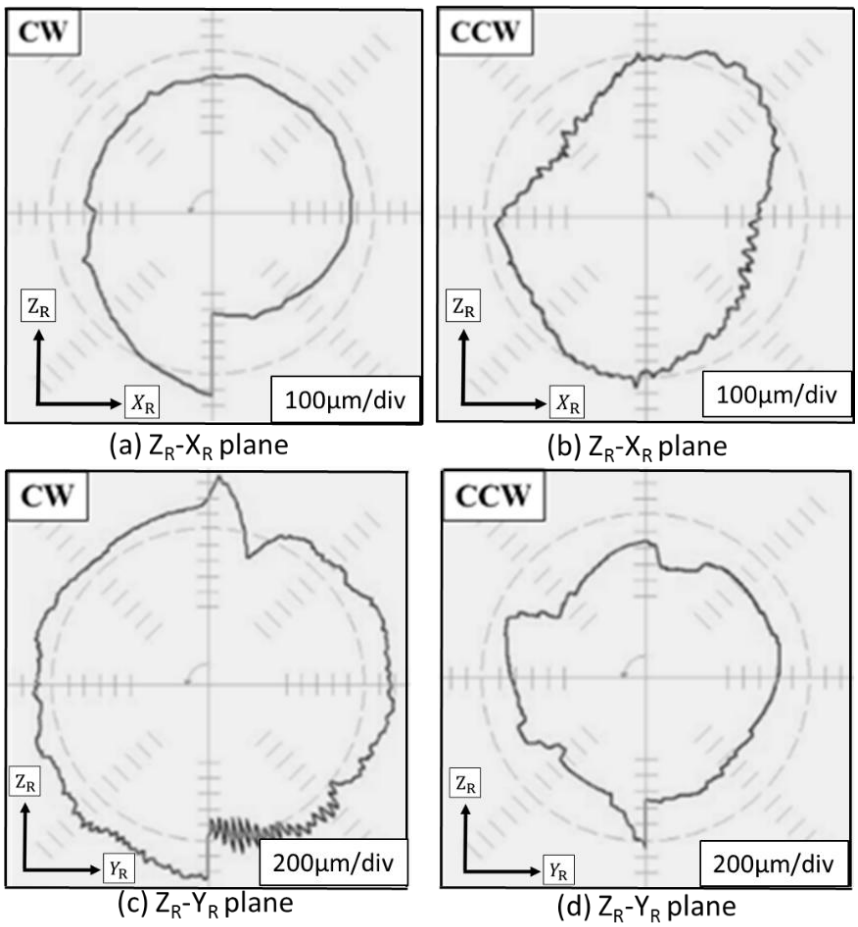

Fig. 7. Result by DBB with lower posture (CW, CCW).

It is supposed the point that an error produces about the plane coordinates that Z_R axis is related to when we move a robot arm from Fig.7(a)~(d), up and down discontinuously existing. In addition, we know what a sudden exercise error produces when we send arc interpolation in 500 forwarding speed mm/min when we let it exercise and send it from data in case of 2000 speed mm/min and raise speed. For the factor of such the motion error, backlash depending at the time of motion of motor inversion of each joint part of dual-arm is thought.

4.3 Motion error of revision method based on backlash

Analysis and revision using the DBB method are effective to improve the motion control of the machine tool precision of 3 and 5-axis control. The DBB method measures the radial direction error of the exercise for the circular motion order and improves the frequency response characteristic, which is the soft element of the control system. It also easily diagnoses the error that was caused by the system's hardware characteristics on the spot. In the dual-arm robot, for the order for angle vector P_i (θ_{xi}, θ_{yi}) which was the targeted value, it was thought that the true exercise angle vector P_i' (θ'_{xi}, θ'_{yi}) was not independent of the angle vector P_i (θ_{xi}, θ_{yi}) when we considered the support structure of the plate on which the rotation about the X_m-axis on the basis of a

turn mainly at J1 and J8. Therefore we could express those relations in Eq. (17) when the true exercise angle vector, which was an instruction angle vector, and the output, which the input supposed was linear, was shape-related.

$$\begin{bmatrix}\theta'_{xi}\\ \theta'_{yi}\end{bmatrix} = \begin{bmatrix}\theta_{xi}\\ \theta_{yi}\end{bmatrix} + \begin{bmatrix}\theta'_{xi}-\theta_{xi}\\ \theta'_{yi}-\theta_{yi}\end{bmatrix} = \begin{bmatrix}\theta_{xi}\\ \theta_{yi}\end{bmatrix} + \begin{bmatrix}\Delta\theta_{xi}\\ \Delta\theta_{yi}\end{bmatrix} + \left(\begin{bmatrix}\delta_{mxi}\\ \delta_{myi}\end{bmatrix}\right) = \begin{bmatrix}\theta_{xi}\\ \theta_{yi}\end{bmatrix} + [E]\begin{bmatrix}\theta_{xi}\\ \theta_{yi}\end{bmatrix}$$
$$= \begin{bmatrix}1+\varepsilon_{xxi} & \varepsilon_{xyi}\\ \varepsilon_{yxi} & \varepsilon_{yyi}\end{bmatrix}\begin{bmatrix}\theta_{xi}\\ \theta_{yi}\end{bmatrix}, (i = 1\sim4) \tag{17}$$

The $\Delta\theta_x$ in Eq. (17), $\Delta\theta_y$, angle error, and [E] are the error coefficient lines. Because the backlash error was over Z_R by more than the result of the measurement of the radius error by the DBB method axially, ε = Arc sin(ΔR/ a2) when we converted the error into the rotary angle of the plate and can demand each ingredient of error coefficient line [E] in this way. However, it is difficult to exactly demand the error coefficient line [E] by experiment, and the measurement error (δ_{mxi}, δ_{myi}) needs to be included to show it in expression (17), and the size, was unknown. Therefore, the result was the turns were worse than with the original instruction vector even if the error became worse when we demanded an inverse matrix including an error and an instruction angle vector by expression (17). Therefore, we shifted to the left side of the board and transformed the measurement errors in expression (17) like in expression (18). We supposed the measurement errors were due to the differences between the calculation result and the laboratory finding of expression (17). When we reduced the measurement error, a measurement error of unknown size was included in (θ''_{xi}, θ''_{yi}), but in this way we thought that we could prevent the error expansion due to the inverse matrix calculation. We'll teach the angle by using Eq.18, if we use the dual arm robot.

$$\begin{bmatrix}\theta''_{xi}\\ \theta''_{yi}\end{bmatrix} = \begin{bmatrix}\theta'_{xi}-\delta_{mxi}\\ \theta'_{yi}-\delta_{myi}\end{bmatrix}\begin{bmatrix}1+\varepsilon_{xxi} & \varepsilon_{xyi}\\ \varepsilon_{yxi} & \varepsilon_{yyi}\end{bmatrix}\begin{bmatrix}\theta_{xi}\\ \theta_{yi}\end{bmatrix} \tag{18}$$

4.4 Rolling motion error under various posture.

We explain the condition of the experiment. In the case of the robot upper and lower posture, we installed a gyroscope sensor in the center point of the working plate and performed an experiment (tilting angle $\theta_0 = 3°$, T = 3.3s, T = 1.3s). **Fig. 8** shows the result of a measurement in the case of the lower posture, and **Fig. 9** shows the result of the measurement in the case of the upper posture. The maximum angle is approximately constant with the lower posture, but we could determines the thing that was not constant with the upper posture when we compared Fig. 9 with Fig. 8. It was thought that the backlash error occurred in the case of the upper posture when compared with the lower posture as a cause of the error in the DBB method. Therefore, in particular, we discuss about the upper posture of the dual arm robot. In addition, from Fig. 7 and Fig. 9, a task was performed where the discontinuous error on the Z_R-axis is produced in the plane in which the Z_R-axis is related, which is the greatest factor of the exercise error in the backlash at the time of the exercise inversion. It becomes the main factor of the error in the circus movement based on the rolling motion of the left-right arm inversion aspect.

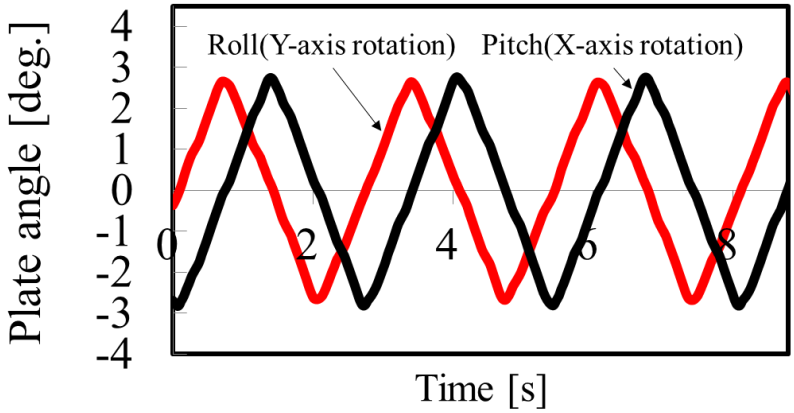

Fig. 8. θ_x-θ_y graph with lower posture.

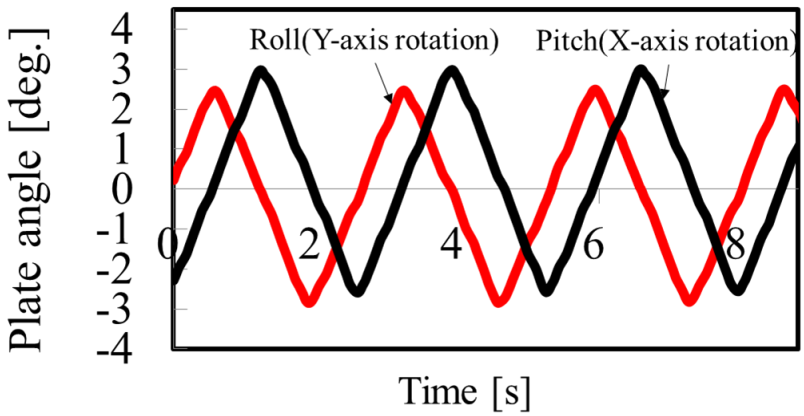

Fig. 9. θ_x-θ_y graph with upper posture.

4.5 Creation of revision method about rolling motion error.

We discuss about the upper posture of the dual arm robot. The greatest radius error when we set the upper attitude was an error produced in particular Fig. 8, 9 by right arm fixation as a specific example. We changed the speed and we showed the case of CW (**Fig. 10**) and the case of CCW (**Fig. 11**). The Fig.10 and Fig.11 show the calculation result of the error coefficient for instruction point. Similarly, we can demand the other elements of the error coefficient matrix.

From these figures, we request a concrete error coefficient line. As an example, we take ε_{xx1} and ε_{xy1} in Eq. (16) and explain them. ε_{xx1} is the rotary angle error of the X_m-axis circumference for the order angle of the X_m-axis circumference. The movement to the instruction point turned the left and right arm in the X_m-axis circumference CW. At first, we used Fig. 10 because it is CW. In addition, we read the data of the Y_R-Z_R plane because it is the turn of the X_m-axis circumference.

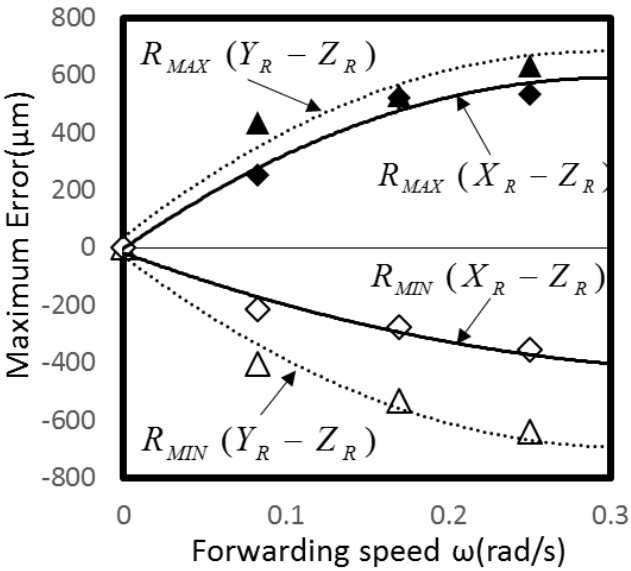

Fig. 10. *Effect of operating speed with upper posture (CW).*

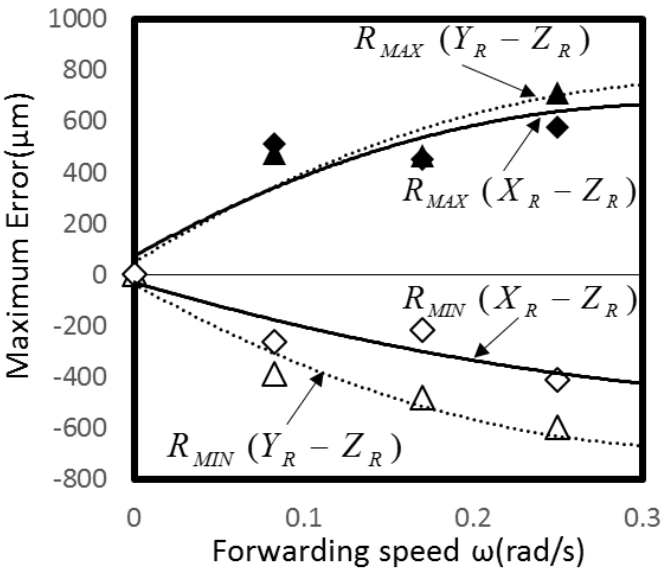

Fig. 11. *Effect of operating speed with upper posture (CCW).*

From a figure, we read the maximum radius error of the left and right arm, and ε_{xx1} was demanded when exchanging the difference of both values of ΔR_{MAX} to the rotary error of the plate. Then, we explained the requests of ε_{xy1}, which was an interaction. Regarding the cause of the interaction, we thought that the backlash due to the Y_m-axis circumference gave an error for the turn of the same X_m-axis rotation. Therefore, the quantity of the backlash (Y_R-Z_R plane) of the Y_m-axis circumference thinks that the difference of ΔR_{MIN} effects appear to the X_m-axis circumference (X_R-Z_R plane) and the

opposite direction and we converted the difference into the turn angle of the plate and used it.

Then, the true instruction angle (θ''_{xi}, θ''_{yi}) of each instruction point was calculated when we substituted the targeted value (θ_{xi}, θ_{yi}) for Eq. (18). In other words, if an error occurred because of the DBB method near the posture that the plate support is expected beforehand, we made the error coefficient line [E] like in the statement above in total in the turn period of the ball, and it was thought that the greatest angle (θ_{xi}, θ_{yi}), which was an aim, was provided when we instructed a true instruction angle (θ''_{xi}, θ''_{yi}). The true instruction angle ($\theta''_{x}i$, θ''_{yi}) can calculate by Eq. (19). Therefore, by proposed method, a true teaching angle to revise the exercise precision was backlash in the dual-arm robot's motion and the motion precision greatly decreased.

$$\begin{bmatrix} \theta''_{xi} \\ \theta''_{yi} \end{bmatrix} = \begin{bmatrix} 1+\varepsilon_{xxi} & \varepsilon_{xyi} \\ \varepsilon_{yxi} & \varepsilon_{yyi} \end{bmatrix}^{-1} \begin{bmatrix} \theta_{xi} \\ \theta_{yi} \end{bmatrix}, (i = 1\sim4) \tag{19}$$

5. CONCLUSION

In this paper, we discussed about the investigation of two-axis synchronous accuracy of plate pivot control with various poses of industrial dual arm robot for ball-rolling motion on working plate. We have proposed a new method for simple, on-site evaluation of motion error in two-axis synchronous rotational motion by inducing a circular rolling motion of a ball on a working plate and measuring the error of the rolling or the error of the ball rolling relative to a reference circle. In this report, we further investigated the motion control of the working plate supported with a dual-arm robot under various postures, in particular, upper and lower posture.

(1) Factor of the robots that have an effect include the end-effecter of the dual-arm robot to handle a plate. It was regarded that the master arm of the robot was at the position where the state of the end-effecter was more asymmetrical than the relations of the slave arm, and we therefore knew the movement of the produced origin position.

(2) As a result, in the plane coordinates that the Z_R-axis was related to by the DBB method, I knew what a particularly discontinuous error would be produced on the Z_R-axis. It is thought the cause was the backlash error depended on the time of motion of motor inversion of each joint.

(3) We held a working plate that was a standard at the top and bottom position and accomplished rolling motion of the ball by plate turning. As a result, the top and bottom maintenance system understood that the effect of the motor backlash became significant.

REFERENCES

[1] Shibukawa T. et al., 1997, "Parallel Mechanism Based Milling Machine," Journal of the Japan Society for Precision Engineering, Vol. 63, No. 12, pp.1671-1675 (In Japanese)

[2] N. Furuya, et al., “A Study on the Improvement of the SCARA Robot Motion,” J. of the Japan Society for Precision Engineering, Vol.54, No.5, pp. 173-178, 1988. (In Japanese)

[3] M. Shiraishi, et al., “High Accuracy Positioning in SCARA-Type Robot by Sensor-based Decoupling Control,” ASME J. of Manufacturing Science and Engineering, Vol.122, Issue 1, pp. 166-173, 1999.

[4] M.Nakagawa, et al., “A Study on the Improvement of Motion Accuracy of Hexapod Type Parallel Mechanism Machine Tool (1st Re- port): The Method of Kinematic Calibration without Gravitation Deformation,” J. of the Japan Society for Precision Engineering, Vol.67, No.8, pp. 1333-1337, 2001. (In Japanese)

[5] Y. Kakino, et al., “Study on the Motion Accuracy of NC Ma- chine Tools (1st Report): The Measurement and Evaluation of Motion Errors by Double Ball Bar Test,” Trans. of the Japan Society of Mechanical Engineers, Vol.52, No.7, pp. 1193-1198, 1986. (In Japanese)

[6] Y. Kakino, et al., “A Study on the Motion Accuracy of NC Machine Tools (2nd Report): Diagnosis of Motion Error Origins by Using Double Ball Bar Test,” Trans. of the Japan Society of Mechanical Engineers, Vol.52, No.10, pp. 1739-1745, 1986. (In Japanese)

[7] Wei WU, Toshiki HIROGAKI and Eiichi AOYAMA, “Motion Control of Rolling Ball by Operating the Working Plate with a Dual-arm Robot,” *International Journal of Automation Technology*, Vol.6, No.1 (2012), pp.75-83.

[8] Wei WU, Toshiki HIROGAKI and Eiichi AOYAMA, “Investigation of Synchronous Accuracy of Dual Arm Motion of Industrial Robot,” Journal of Key Engineering Materials, Vol.516. (2012) ,pp.234-239.

[9] S. Awtar et al., Mechatronic design of a ball-on-plate balancing system”, Mechatronics, Vol.12, No. 2, (2002), pp. 217-228

[10] Wei WU, Shun KINOSHITA, Toshiki HIROGAKI and Eiichi AOYAMA, “Detection of Motion Error Under Synchronous Two-Axis Control of a Dual Arm Robot Based on Monitoring of Ball Rolling Motion on a Plate,” Journal of Key Automation Technology, Vol.9, No.1 (2015) , pp.33-42.